Integrative and Comparative Biology

Integrative and Comparative Biology, volume 54, number 6, pp. 1034–1042
doi:10.1093/icb/icu026

Society for Integrative and Comparative Biology

SYMPOSIUM

Self-burial Mechanics of Hygroscopically Responsive Awns

Wonjong Jung,* Wonjung Kim[1,†] and Ho-Young Kim[2,*]

*Department of Mechanical and Aerospace Engineering, Seoul National University, Seoul 151-744, Korea; †Department of Mechanical Engineering, Sogang University, Seoul 121-742, Korea

From the symposium "Shaking, Dripping, and Drinking: Surface Tension Phenomena in Organismal Biology" presented at the annual meeting of the Society for Integrative and Comparative Biology, January 3–7, 2014 at Austin, Texas.

[1]E-mail: wonjungkim@sogang.ac.kr
[2]E-mail: hyk@snu.ac.kr

Synopsis We present the results of a combined experimental and theoretical investigation of the mechanics of self-burial of some plant seeds whose morphologies respond to environmental changes in humidity. The seeds of *Erodium* and *Pelargonium* have hygroscopically responsive awns that play a critical role in their self-burial into soil. The awn, coiled in a dry state, uncoils to stretch linearly under highly humid condition because of a tilted arrangement of cellulose microfibrils in one of the layers of the awn's bilayered structure. By measuring the mechanical characteristics of the awns of *Pelargonium carnosum*, we find that the extensional force of the awn can be aptly modeled by the theory of elasticity for a coiled spring. We further show that although the resistance to the seed-head penetrating relatively coarse soils without spinning is large enough to block the digging seed, the rotation of the seed greatly reduces the soil's resistance down to a level the awn can easily overcome. Our mechanical analysis reveals that the self-burial of the seed is a sophisticated outcome of the helically coiled configuration of the awn.

Introduction

Plants can generate motions and deformations, that our eyes often fail to catch, in response to various stimuli such as light, heat, gravity, and change in humidity. Slow movements of plants are evidenced by twirling circumnutation of growing tendrils (Gerbode et al. 2012) and blooming flowers (Reyssat and Mahadevan 2009), whereas motions rapid enough to notice include dispersal of seeds of Dwarf mistletoe (Hinds and Hawksworth 1965), folding of *Mimosa* leaves (Weintraub 1952), and snapping of Venus flytraps (Forterre et al. 2005). A remarkable common feature in strategies of these motions is that they do not rely on complicated protein structures like muscles. Instead, most botanical movements are hydraulic in nature—that is, simple transport of fluid consisting mostly of water into and out of plant tissue generates motions. Also, such motions are often triggered by supply or deprival of water either in the form of liquid or vapor.

A common example of water-driven botanical deformation is the opening and closing of pine cones in response to environmental changes in humidity, whose mimic was built by layering hygroscopically active and inactive films (Reyssat and Mahadevan 2009). It is now widely known that seeds and spores of some plant and fungus species are explosively launched into the air as their ovaries and sporophores, respectively, become exceedingly dry and crack open (Beer and Swaine 1977; Skotheim and Mahadevan 2005; Dumais and Forterre 2012). A pair of awns of wild wheat (*Triticum turgidum* ssp. *dicoccoides*) repeatedly open and close on the ground in response to variation of the soil's moisture content, which is a remarkable motion seeds employ in self-burial (Elbaum et al. 2007). Ma et al. (2013) showed that an engineered, hygroscopically active polymer film can be actuated by a humidity gradient in the surrounding air, just as are the awns of wild wheat. This process potentially can be used to generate electricity if piezoelectric properties are effectively combined.

Among various kinds of botanical motilities driven by change in humidity, here we aim to analyze the motions of seeds of some species of the genera *Erodium* and *Pelargonium*. It was revealed several decades ago that the seed of *Erodium cicutarium* has a

Advanced Access publication April 23, 2014

helical awn that spontaneously uncoils when wet but re-coils when dry (Stamp 1984). Such hygroscopic characteristics are known to play a critical role both in dispersal and germination of seeds. In a dry season, the seeds of *E. cicutarium*, confined in straight configuration in an ovary, are explosively launched into air as the ovary shell cracks due to low humidity. The mechanical energy stored in the awn is released rapidly as it coils to turn to its natural shape when in the dry state. A physical model of this process was developed by Evangelista et al. (2011). The helical configuration of dry *E. cicutarium* seeds was mathematically described using a non-euclidean rod-model by Aharoni et al. (2012). Upon landing, the seeds screw into the ground with the coiling and uncoiling cycle of the awn, a self-burial behavior different from that of wild wheat.

The awns of *Pelargonium*, another genus of the family Geraniaceae, to which *Erodium* belongs, also coil and uncoil in response to changes in humidity as demonstrated by a seed of *Pelargonium carnosum* in Fig. 1A. However, the awns of *Pelargonium* typically are thinner and softer than those of *Erodium* species. It is because their seeds become airborne by lift from wind rather than being catapulted like *Erodium* seeds (Abraham and Elbaum 2013b). Thus, the seeds of *Pelargonium* are relatively light and covered with feather-like hairs, so that the seeds serve as parachutes when dry (Fig. 1B). Therefore, the helical motion itself does not drive the release of the seeds in *Pelargonium*. Rather, the helical motion of the awns of *Pelargonium* is mainly used to screw the seeds into ground. Therefore, the microstructure and shape of the seeds of *Pelargonium* are highly likely to have been evolved within the context of self-burial exclusively, not for dispersal.

Below we provide physical accounts of hygroscopically driven botanical movements, which particularly lead to helical coiling and uncoiling of the awns of seeds. We also present experimental results for mechanical properties of some seeds of *Pelargonium* that enable their unique self-burial behavior. Investigating the water-driven helical motion of the awns can contribute to development of micro-robot actuators powered by environmental changes in humidity, as well as advancing and diversifying our understanding of botanical movements.

Mechanisms and geometry of botanical movements

In general, there are two different mechanisms that generate botanical motions or deformations. In some plants, the creation of motion relies on changes in turgor pressure, which is caused by the osmotic flow of water through plasma membranes, as driven by a gradient in concentration of solute. Increased turgor pressure inflates the membrane against the cell wall, thus providing the rigidity of the plant's organ. Plants may actively control solute concentrations and thereby generate motions, such as the opening of stomata (Franks et al. 2001), blooming and wilting of flowers, folding of mimosa leaves, and closing of Venus flytraps. A similar role of turgor pressure can be observed in the kingdom of fungi; fungal spores are ejected from mushrooms due to the osmotic pressure of turgid tissues (Roper et al. 2010).

Besides changes of turgor pressure due to osmosis, many motions of plants are caused by volumetric change owing to the hygroscopic nature of some constituent materials. The wall of plant cells is a composite made up of cellulose microfibrils and the soft matrix of structured polysaccharides, hemicellulose, soluble proteins, and other substances. The soft matrix inside the cell walls expands when it combines with molecules of water. Hygroscopic materials generally have hydrophilic moiety, allowing water molecules to be stored between intermolecular chains or networks via hydrogen bonding. The volume between intermolecular chains or networks increases as they become impregnated by water molecules, leading to swelling of wet tissues. Because the combination with water molecules is reversible, the plant's swollen tissue can shrink back to its original size when dry. Such hygroscopic response is responsible for the opening of pine cones (Reyssat and Mahadevan 2009), self-sealing of pollen grains (Katifori et al. 2010), opening of seed pods (Armon et al. 2011), and self-burial of the awns of wild wheat (Elbaum et al. 2007) and *Erodium* seeds (Stamp 1984).

The geometry of deformed plant tissues after hygroscopic expansion is often determined by the arrangement of microfibrils, fiber-like strands consisting of glycoproteins and cellulose. Because the water-driven swelling of plant cell walls occurs in the hygroscopic soft matrix between crystalline cellulose fibril, the direction of the hygroscopic swelling is perpendicular to the orientation of cellulose microfibrils. Attaching multiple layers of differently arranged microfibrils can yield bending or twisting of the structure. Indeed, hygroscopic tissues found in awns of wild wheat, *Erodium* and *Pelargonium* seeds typically consist of multiple layers with different orientations of their microfibrils.

The awns of wild wheat consist of two layers, called a ridge layer and a cap layer. While a ridge layer has randomly oriented cellulose microfibrils, in

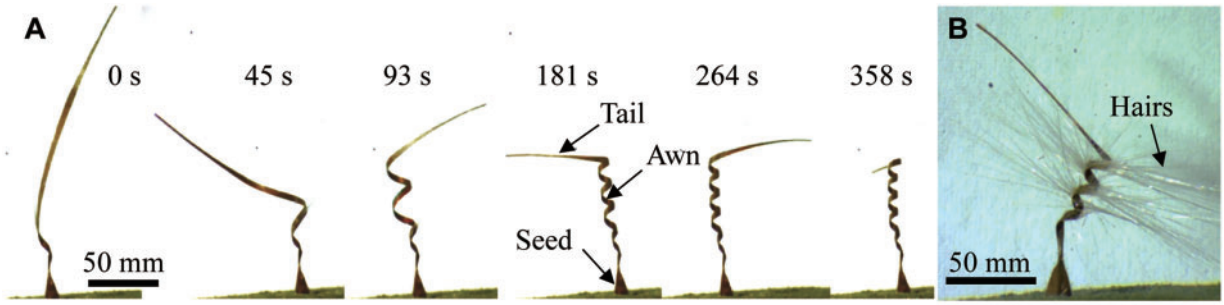

Fig. 1 (**A**) Helical coiling of an awn of *Pelargonium carnosum* that is dried at room temperature from the initially wet, straight configuration. (**B**) A parachute-like shape of a *P. hortorum* seed with hairs.

the cap layer the cellulose microfibrils are well aligned along the long axis of the cell (Elbaum et al. 2007, 2008). Because the direction of primary expansion is orthogonal to the arrangement of cellulose microfibrils, the ridge and cap layers have a longitudinal expansion and a two-directional expansion in a plane, respectively. The difference in expansion causes the bending of the awn, which repeats as the environmental humidity changes. This motion enables the seed to employ silicified ratchets to dig into the soil and to find a place advantageous for germination.

The awns of *Erodium* and *Pelargonium* exhibit deformation distinguished from that of wild wheat by coiling helically rather than merely bending. A fully wet awn of *E. cicutarium* is straight, but it transforms to a helical coil when dry. The helical configuration is defined by the microfibril angle (MFA), the angle between the long axis of the plant cell and the axis perpendicular to the plane formed by the microfibrils (Barnett and Bonham 2004). Because the cell wall contracts in a direction essentially perpendicular to the plane formed by the microfibrils, the direction of contraction is determined by the MFA (Fratzl et al. 2008). When cellulose microfibrils are helically coiled along the plant cell at a tilted angle, hygroscopic deformation induces twisting as well as bending (Abraham et al. 2012; Abraham and Elbaum 2013a). In the inner layer of the *E. cicutarium* awn, cells with a tilted MFA cluster together, whereas the axis perpendicular to the plane formed by microfibrils is arranged along the long axis of the cell in the outer layer. Therefore, changes in humidity induce coiling motions, which are useful for the self-burial of seeds. Many members of the family Geraniaceae, including *Erodium* and *Pelargonium*, have a variety of configurations depending on the combination of layers with a particular MFA (Abraham and Elbaum 2013b). The inner layer of the awn of *Pelargonium* is shown in Fig. 2.

Theory of how force is generated by self-burying seeds

To investigate the forces generated by self-burying seeds, we begin with a brief description of the mechanics of the bending of a beam (Landau and Lifshitz 1970). When loads are applied to a straight beam in the direction perpendicular to the longitudinal axis of the beam, the beam bends in a curve. A curve can be geometrically described in terms of curvature κ or the radius of curvature $\rho = 1/\kappa$. Because bending a straight beam induces the relative rotation $d\theta$ of two cross-sections that are separated by an infinitesimal distance ds as shown in Fig. 3, we get $ds = \rho d\theta$. The strain ε, the ratio of the elongated length to the original length, depends on the distance y from the neutral surface in which longitudinal lines do not change in length, such that $\varepsilon \approx \kappa y$.

The relationship between the curvature and loads can be deduced by the strain–stress relationship in elastic material: Hooke's law. In elementary solid mechanics, the moment-curvature relation is given by $M = EI\kappa$, where M is the local bending moment produced by the external loads, E is Young's modulus, and I is the area moment of inertia. Note that bending stiffness EI is given by a combination of material property E and geometric characteristic I that depends on the cross-sectional shape of the beam. A beam with a rectangular cross-section has $I = bh^3/12$, where b and h are the width and the height of the cross-section, respectively. If a beam is originally curved, the applied moments produce the change in curvature, such that $M = EI\Delta\kappa$ when a small deflection is assumed.

The curvature of hygroscopic awns may change via the spatial variation of the degree of expansion. When two different layers of an awn differ in strain $\Delta\varepsilon$ after hygroscopic expansion, the curvature is given by $\kappa \sim \Delta\varepsilon/t$, where t is the characteristic thickness of the awn. As deformation of one layer is restricted by the other, the difference in curvature

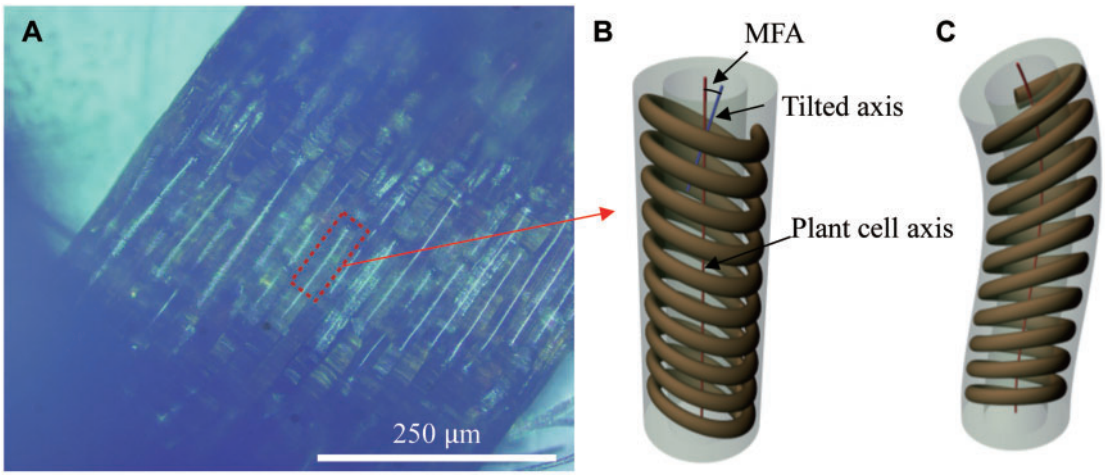

Fig. 2 The optical image of the inner layer of the awn of a *Pelargonium canosum* seed (**A**). The schematic illustration of a tilted helix of microfibril along the plant cell, depicted as in Fig. 5 of Abraham et al. (2012) (**B**). Bending and twisting occur in the awn as it dries (**C**).

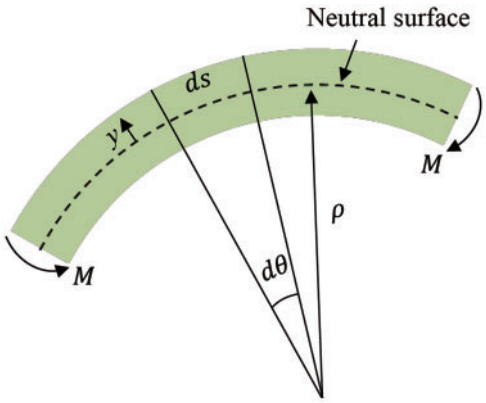

Fig. 3 A beam subjected to a bending moment *M*.

between the natural and restricted configurations, $\Delta\kappa$, results in a bending moment on the other layer. Although a beam consisting of two rectangular layers with uniform cross-sections exhibits two-dimensional deformation, a beam of two non-rectangular layers can bend in a three-dimensional fashion because of asymmetry in deformation. Jeong et al. (2011) demonstrated that a planar structure with a sloped bilayer is bent as well as twisted when one of the layers is asymmetrically expanded. Because the ratio of two layers varies with the distance b along the depth of the cross-section, the curvature is a function of b, which results in a three-dimensional deformation (see Fig. 4A).

In the case of the awns of *Erodium* and *Pelargonium* seeds, a single layer, referred to as an inner layer, consists of a number of cells, each of which is capable of bending and twisting as shown in Fig. 4. The soft matrix of the cell wall contracts when dry, but the cell wall is wound around by hygroscopically inactive microfibrils. Therefore, the cell can contract only in the direction perpendicular to the plane formed by the rotation of microfibrils (Fratzl et al. 2008). Because the direction of contraction does not coincide with the long axis of the cell, the cell must bend and twist while drying. A simple hybrid beam is shown in Fig. 4 and the cells of interest here share a common feature in that they coil due to different hygroscopic responses of the two constituent materials. The difference lies in the spatial arrangement of the materials—the simple hybrid beam has completely separated layers of hygroscopically active and inactive materials, whereas the hygroscopically inactive microfibrils are embedded in and twined around the hygroactive materials of the cell. The helical deformation of the inner layer of the awn is the collective outcome of its constituent cells' deformations. On the other hand, the outer layer contributes to the coiling of the awn but slightly because its cells have smaller MFA than the inner layer. Therefore, the inner layer plays a pivotal role in the helical deformation of the awn whereas the outer layer passively modifies the degree of deformation (Abraham et al. 2012).

Coiling and uncoiling of the awns of *Erodium* and *Pelargonium* seeds result in rotation and consequent digging by the seeds. Digging arises from two different mechanical effects: force due to coil expansion and torque due to awn-tail rotation. The forces are exerted against a support provided by pebbles or bark of trees in nature (Stamp 1984), as schematically illustrated in Fig. 5. Uncoiling of a helical structure into a straight configuration leads to a change in length along the axis of the helix, and thrust (P) is

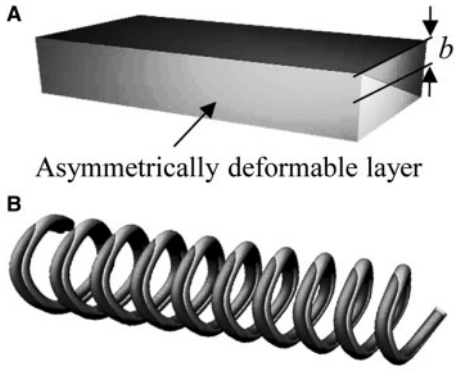

Fig. 4 A bilayer with asymmetrically deformable layer (**A**). Shrinking and consequent twisting in a spiral of the bilayer (**B**). The figures were depicted as in Fig. 3 of Jeong et al. (2011).

exerted normal to the surface of the soil. In addition, the relative rotation of the helical structure to the tip of the long tail produces torques ($M = rT$). The thrust and torque together are responsible for self-burial of the seed.

The order of magnitude of force generated by the coiling deformation can be estimated from a coiled-spring model. For a linear coil spring with rectangular cross-section, the displacement δ under axial loading P is given by $\delta \sim PlD^2/(EI)$, where l is the length of the active wire of the spring (the length of the gray line in Fig. 5) and D is the diameter of the coil (Wahl 1963). Therefore, the spring constant K, i.e., loading per unit displacement, is estimated as

$$\mathrm{K} \sim EI\kappa^2/l. \quad (1)$$

We see that the coil can generate a larger force (higher K) with the same displacement as the coil becomes stiffer, thicker, more highly curved and shorter. One should note that while the linear coil spring model assumes constant E, I, and curvature, and thus a constant moment along the length, the actual awn experiences changes in E, I and curvature both spatially and temporally as the environmental humidity varies. More sophisticated models, for example a logarithmic spiral model for a helix (Evangelista et al. 2011) and a variable stiffness model due to moisture diffusion in the tissue (Reyssat and Mahadevan 2009), can allow us to predict the spring force of the awn more accurately, which we do not pursue further here. For the seed to dig into the ground, the thrust generated by the helical coil should overcome the resistance of the soil to penetration. Below, we experimentally measure the forces produced by the self-burying seeds and compare the results with both the theoretical values and the soil's resistance.

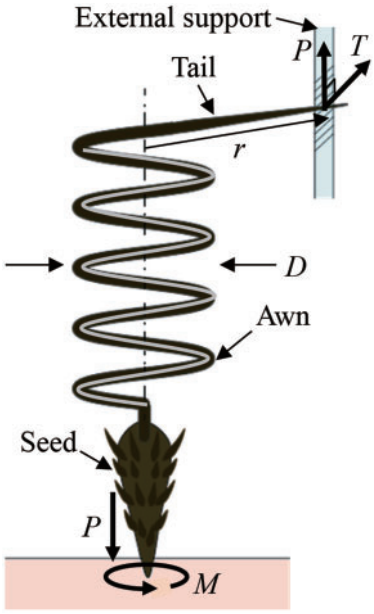

Fig. 5 Geometry and forces of a seed with a helically coiled awn digging into soil. The arrows of P and T are perpendicular to each other.

Materials and methods

The seeds of *P. carnosum*

The seeds were purchased from a nursery (Phoenix Desert Nursery) in AZ, USA, and their shapes are displayed in Fig. 6. The SEM image (Fig. 6B) was taken after sputter-coating the specimen with Pt. In the following, we present the average values of the seeds' dimensions through measurements of n specimens. The seed head of *P. carnosum* is 5.3 ± 0.3 mm long and the tail length of the awn is 19.5 ± 1.3 mm ($n = 3$). The end-to-end distance of dried awn $l_\mathrm{d} = 8.7 \pm 0.3$ mm, the length of wet awn $l = 15.0 \pm 1.3$ mm, the maximum width of the awn $b = 531 \pm 66\,\mu$m, and the height of the cross-section of the awn $h = 51 \pm 7.6\,\mu$m ($n = 3$), when hairs were removed before measurement. The maximum coil diameter of the awn is $D = 1.0 \pm 0.2$ mm, the mass of seed without hairs is 4.3 ± 0.5 mg, and the number of turns in a completely dried state is 7 ± 1 ($n = 10$). Assuming that Young's modulus of the awn of *P. carnosum* to be similar to that of wood in a direction parallel to the grain, $E \sim 9$ GPa (Ashby and Jones 2005), the spring constant K of the awn of *P. carnosum* seeds is estimated from Equation (1) to be $\sim$12.5 N/m. Here, we used $I = bh^3/12 = 5.2 \times 10^{-18}\,\mathrm{m}^4$ and $\kappa = 2/D = 2 \times 10^3\,\mathrm{m}^{-1}$.

The measurement of forces generated by the awn

In order to measure the forces generated by the deformation of the awn, we used a load cell originally

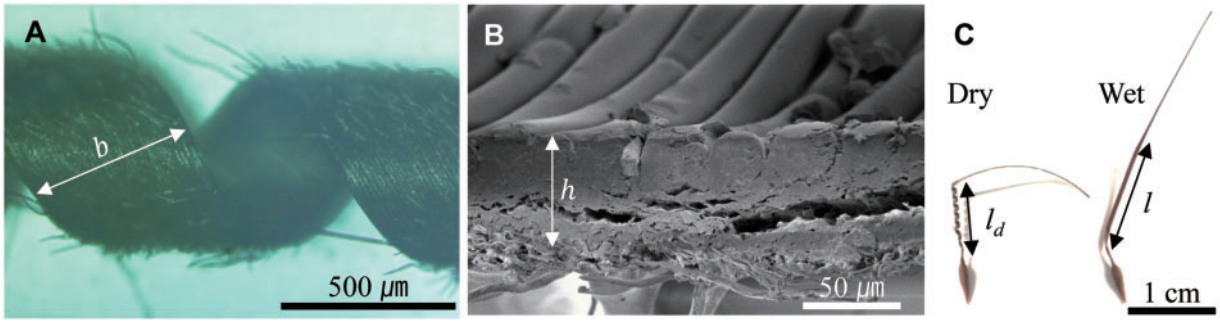

Fig. 6 The awn of *Pelargonium carnosum*. (**A**) Optical micrograph of the coiled awn. (**B**) SEM image of the cross-section. (**C**) Optical images of the seed in dry and wet states.

intended for measurement of dynamic contact angle (DCAT 21, DataPhysics instruments GmbH). Humidity around the awn was increased by supplying vapor in the surrounding air with a commercial humidifier. One end of the awn was fixed to an external support, and the other (free) end was located within 1 mm from the load cell (Figs. 7A and 8A). As we increased humidity, the initially free end of the awn touched and pushed the load cell. The extensional force was measured by constraining the increase in length as shown in Fig. 7A and the torque was measured by obstructing the rotation as shown in Fig. 8A. The forces produced by three different awns of *P. carnosum* were measured in each measurement. The scatter in the values of measurements among the specimens was at most ±50% from the data of the specimen shown following. Since we are interested in obtaining estimates of the forces generated by the awn, only to the order of magnitude, the observed variability of the force data does not invalidate the simple mechanical model constructed in this work.

The measurement of force required for digging

In order to measure the thrust forces required for the seed of *P. carnosum* to dig into soil, we also used the load cell system of DCAT 21. Various sizes of glass beads (SiLibeads®, Sigmund Linder GmbH) were used to mimic the soils in nature. One end of the seed head was fixed to the load cell and a beaker containing the glass beads moved against the seed with a constant velocity, of 0.05 mm/s (Fig. 9A). In experiments to measure the thrust forces during rotation of the seed, we rotated the beaker at 7 rpm while maintaining the linear constant speed of 0.05 mm/s. This corresponds to the advance of the seed by the length of the seed head after 7 revolutions (equal to the number of turns of the awn). Five different seed heads were used for the measurement. The scatter of the values of the measurements among the specimens was at most ±50% from the data for the specimen shown here.

Experimental results

The forces produced by three awns of *P. carnosum* were measured as shown in Fig. 7A. Figure 7B presents representative measurements of the forces with respect to time. As the awn rotates during expansion, the contact of the end of the awn with the load cell is periodically loosened. Thus, the force measured by the load cell shows multiple peaks. The force peak reached at ∼40 s is ∼3.2 mN, at which instant the axial displacement is measured to be 0.5 mm. Although the awn stretches until the axial extension reaches ∼6 mm (Fig. 7B), the thrust does not monotonically increase with the extension. It is because Young's modulus dramatically decreases as the plant tissue becomes wet (Hepworth and Vincent 1998) and the awn buckles when stretched exceedingly. The thrust predicted by the coiled-spring model when δ is 0.5 mm is $P = K\delta \sim 6$ mN, a value in reasonable agreement with the experimental measurement.

The deformation of the awn of *P. carnosum* produces rotational motion in addition to the axial expansion. When the awn's tail is fixed by an external means, the uncoiling motion of the awn induces the rotation of the head of the seed. We experimentally measured the torque exerted by the end of an awn of *P. carnosum* (Fig. 8A) as it rotates with the increase of humidity. Figure 8B shows that the force is measured by the load cell in a cyclical manner because the awn periodically loses contact with the sensor because of rotation. The representative data indicate that the maximum force produced by the awn's rotation is ∼1 mN, the same order of magnitude as the extensional force. The peaks of the force decrease in magnitude with time, as consistent with the tendency observed in Fig. 7B, because of the decrease of

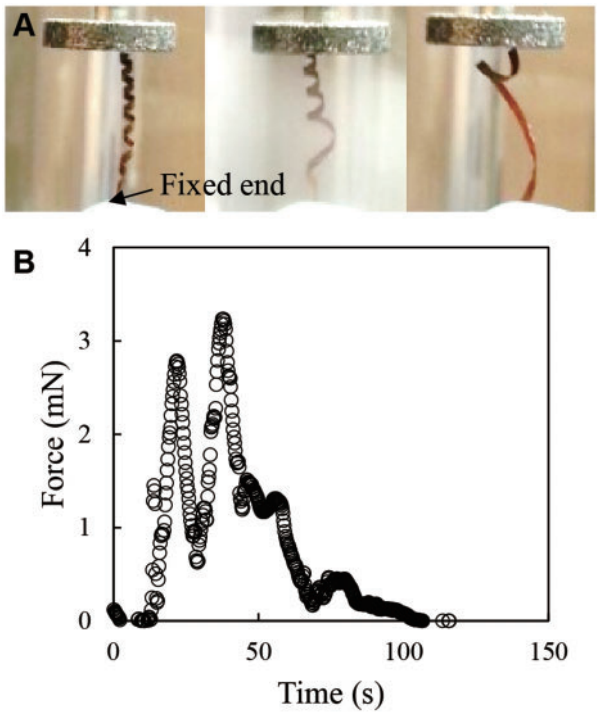

Fig. 7 (**A**) Experimental set-up to measure the extension force of the awn of *Pelargonium carnosum*. (**B**) Measurements of the extension force.

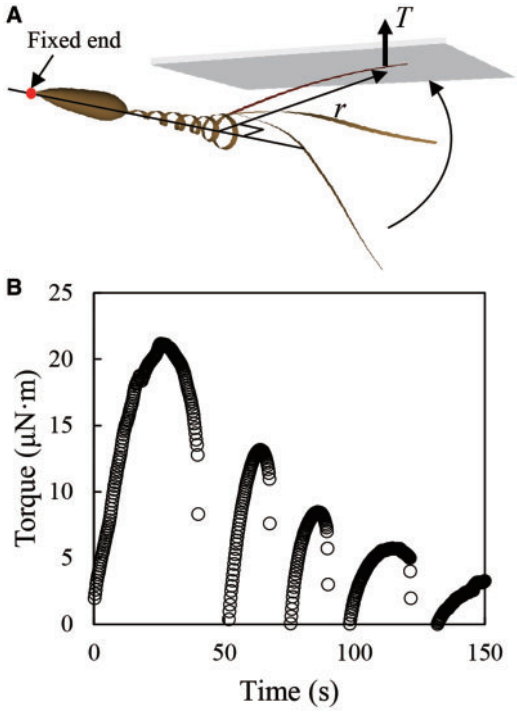

Fig. 8 (**A**) Experimental set-up to measure torque induced by rotation of the awn's tail. (**B**) Measurements of the force exerted on the load cell during rotation of the awn's tail.

Young's modulus with increasing water content in the awn's tissue. The length of the tail corresponds to the moment arm, which measures 20 mm, and thus the maximum torque generated by the hygroscopic deformation is on the order of 20 μN m.

We now consider whether the forces generated by the awn are strong enough to enable the seeds to dig into soil. To this end, we measured the forces required for the seeds to dig into soils of different sizes of grains. As model soils, we used glass beads with average diameters of 0.25, 0.83, and 1.40 mm, which represent typical sands of fine, medium, and coarse grains, respectively (Wentworth 1922). The force exerted by the seed on the soil was measured as a function of the distance the seed moved into the soil. Figure 9C shows that the force (filled symbols) tends to increase almost linearly with the displacement of glass beads of an average diameter of 0.25 mm. As the seed travels 4 mm into the soil, a typical length of the head of the seed as shown in Fig. 9B, the force increases to ~3 mN, a typical value of the maximum extension force of the uncoiling awn. For larger beads (Figs. 9D and E), the forces periodically peak and drop, supposedly because of the jamming and relaxation of the glass beads that interact with the seed-head of similar transverse diameter as that of the bead. We see that the measured peak forces in the glass beads increase with the size of bead, so that the peak force is ~5 and 7 mN for glass beads with an average diameter of 0.83 and 1.40 mm, respectively. Considering that the maximum force arising from the extension of the awn spring is typically <3 mN, the linear translation of the seed into soils of relatively large grains is likely to be severely blocked by the soil's resistance.

The most remarkable difference between the self-burial behavior of *Erodium* and *Pelargonium* seeds and that of wild wheat is that they rotate, or screw into ground with helically coiled awns. Therefore, we quantify the effects of rotation during digging of the seeds by rotating the soil container while it is being raised. Figure 9C–E shows that the resistance of the soil against the penetrating seed is greatly reduced when the seed rotates (empty symbols), so that the force needed to push the seed into the ground is much less than the maximum extension force of the awn spring. These experiments show that the rotation greatly eases the seed's penetration into soil. For beads of average diameters of 0.25, 0.83, and 1.40 mm, rotation reduces the maximum forces experienced by the seed by 75%, 70%, and 73%, respectively. This reduction is sufficient that the extension of the awn spring overcomes the soil's resistance. It is interesting to note that an analogous

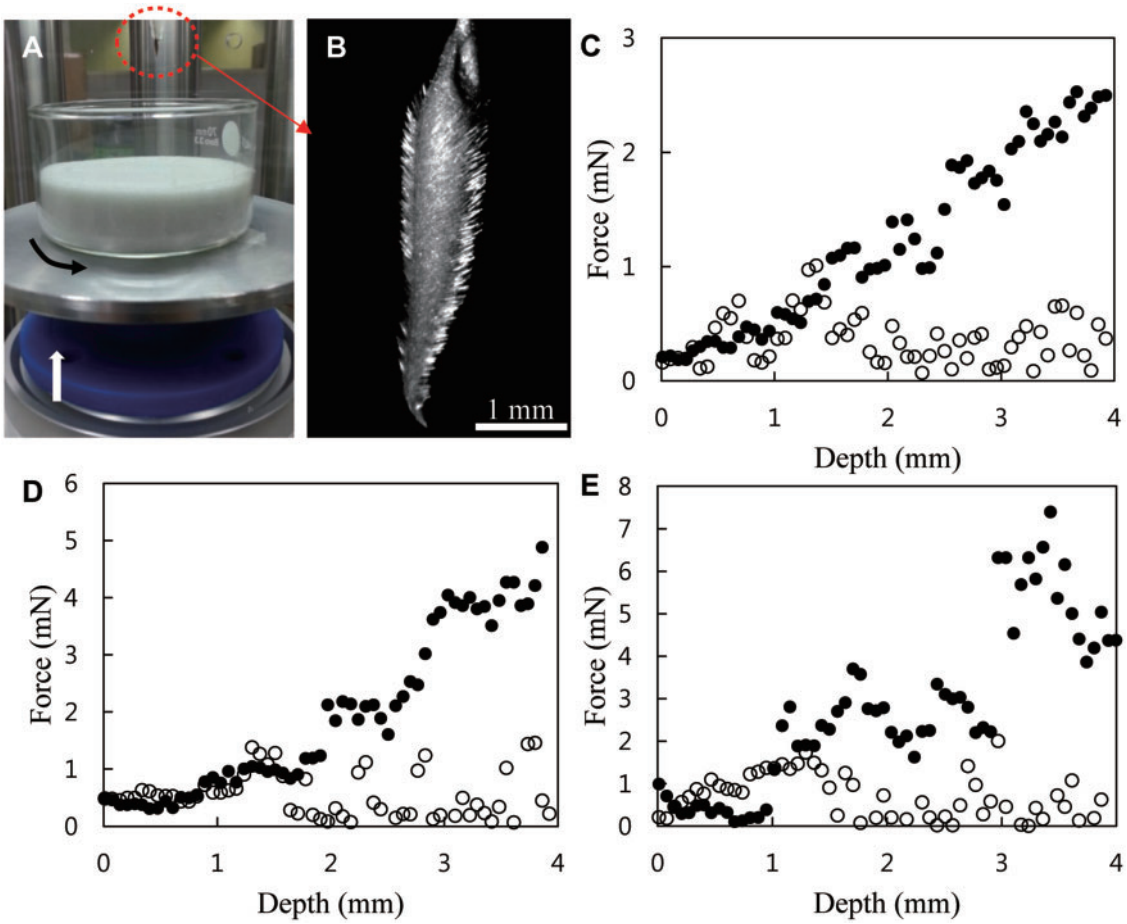

Fig. 9 (**A**) Experimental measurement of the resistance of soil against penetration of a seed (enclosed in a red circle). (**B**) Optical micrograph of the head of a *Pelargonium carnosum* seed. The lower end touches soil. Measurements of the force exerted by the seed on the glass beads as a function of the distance the seed moves into the beads with an average diameter of 0.25 (**C**), 0.83 (**D**), and 1.40 mm (**E**). The filled and empty symbols correspond to the forces of the unspinning and spinning seeds, respectively.

mechanism is employed by Atlantic razor clams (*Ensis directus*) that burrow into sand via local fluidization caused by the motion of their valves (Winter et al. 2012).

Conclusions

In this work, we have provided physical accounts of hygroscopically driven botanical movements, which particularly lead to helical coiling and uncoiling of awns of *Erodium* and *Pelargonium* seeds. We suggest that the observed helical rotation of *Pelargonium* awns in response to environmental changes in humidity is caused by the tilted arrangement of the microfibrils in the inner layer of the awn's cell walls, based on the similarity of the awn's structure to that of *E. cicutarium* awns (Abraham et al. 2012). We have also presented experimental measurements of the mechanical characteristics of *P. carnosum*'s awns that enable self-burial of the seeds in the soil. The extensional force of the awn can be approximately modeled by the theory of elasticity for a coiled spring. Although the resistance to the seed's head penetrating relatively coarse soils without spinning is larger than the extensional force of the awn spring, the rotation of the seed is shown to greatly ease the digging of the seed into soil. Therefore, we may conclude that the awn's hygroscopic coiling, combined with the axial extension and rotation is critical for the success of this self-burial behavior.

Our quantitative measurements of the awn's force and torque, and the soil's resistance, with and without rotation of the seed, naturally led to the question of the detailed mechanism behind the seed-head's rotation giving rise to such dramatic decrease in the forces needed to advance the seed into the soil. The fact that the seed's head is shaped like a cone must assist in self-burial, but whether the cone's angle has been optimized for such screwing should be answered by further research. The water-driven

helical motion of the awns suggests a new actuating mechanism for artificial micro-robots that harness environmental energy associated with changes of humidity in time, or of humidity gradients over space.

Acknowledgment

Administrative support from SNU-IAMD is gratefully acknowledged.

Funding

Grants from Samsung Research Funding Center of Samsung Electronics (SRFC-MA1301-05) and National Research Foundation of Korea (2013034978 and 2013055323).

References

Abraham Y, Elbaum R. 2013a. Quantification of microfibril angle in secondary cell walls at subcellular resolution by means of polarized light microscopy. New Phytol 97:1012–9.

Abraham Y, Elbaum R. 2013b. Hygroscopic movements in Geraniaceae: the structural variations that are responsible for coiling or bending. New Phytol 199:584–94.

Abraham Y, Tamburu C, Klein E, Dunlop JWC, Fratzl P, Raviv U, Elbaum R. 2012. Tilted cellulose arrangement as a novel mechanism for hygroscopic coiling in the stork's bill awn. J R Soc Interface 9:640–7.

Aharoni H, Abraham Y, Elbaum R, Sharon E, Kupferman R. 2012. Emergence of spontaneous twist and curvature in non-euclidean rods: application to Erodium plant cells. Phys Rev Lett 108:238106.

Armon S, Efrati E, Kupferman R, Sharon E. 2011. Geometry and mechanics in the opening of chiral seed pods. Science 333:1726–30.

Ashby MF, Jones DEH. 2005. Engineering material 1. 3rd ed. New York (NY): Elsevier.

Barnett JR, Bonham VA. 2004. Cellulose microfibril angle in the cell wall of wood fibres. Biol Rev 79:461–72.

Beer T, Swaine MD. 1977. On the theory of explosively dispersed seeds. New Phytol 78:681–94.

Dumais J, Forterre Y. 2012. "Vegetable dynamicks": the role of water in plant movements. Annu Rev Fluid Mech 44:453–78.

Elbaum R, Zaltzman L, Burgert I, Fratzl P. 2007. The role of wheat awns I the seed dispersal unit. Science 316:884–6.

Elbaum R, Gorb S, Fratzl P. 2008. Structures in the cell wall that enable hygroscopic movement of wheat awns. J Struct Biol 164:101–7.

Evangelista D, Hotton S, Dumais J. 2011. The mechanics of explosive dispersal and self-burial in the seeds of the filaree, *Erodium cicutarium* (Geraniaceae). J Exp Biol 214:521–9.

Forterre Y, Skotheim JM, Dumais J, Mahadevan L. 2005. How the Venus flytrap snaps. Nature 433:421–5.

Franks PJ, Buckley TN, Shope JC, Mott KA. 2001. Guard cell volume and pressure measured concurrently by confocal microscopy and the cell pressure probe. Plant Physiol 125:1577–84.

Fratzl P, Elbaum R, Burgert I. 2008. Cellulose fibrils direct plant organ movements. Faraday Discuss 139:275–82.

Gerbode SJ, Puzey JR, McCormick AG, Mahadevan L. 2012. How the cucumber tendril coils and overwinds. Science 337:1087–91.

Hepworth DG, Vincent JFV. 1998. The mechanical properties of xylem tissue from tobacco plants (*Nicotiana tabacum* 'Samsun'). Ann Bot Lond 81:751–9.

Hinds TE, Hawsworth FG. 1965. Seed dispersal velocity in four dwarfmistletoes. Science 23:517–9.

Jeong KU, Jang JH, Kim DY, Nah C, Lee JH, Lee MH, Sun HJ, Wang CL, Cheng SZD, Thomas EL. 2011. Three-dimensional actuators transformed from the programmed two-dimensional structures via bending, twisting and folding mechanisms. J Mater Chem 21:6824–30.

Katifori E, Alben S, Cerda E, Nelson DR, Dumais J. 2010. Foldable structures and the natural design of pollen grains. Proc Natl Acad Sci USA 107:7635–9.

Landau LD, Lifshitz EM. 1970. Theory of elasticity. 2nd ed. New York (NY): Pergamon Press.

Ma M, Guo L, Anderson D, Langer R. 2013. Bio-inspired polymer composite actuator and generator driven by water gradients. Science 339:186–9.

Reyssat E, Mahadevan L. 2009. Hygromorphs: from pine cones to biomimetic bilayers. J R Soc Interface 6:951–7.

Roper M, Seminara A, Bandi MM, Cobb A, Dillard R, Pringle A. 2010. Dispersal of fungal spores on a cooperatively generated wind. Proc Natl Acad Sci USA 107:17474–9.

Skotheim JM, Mahadevan L. 2005. Physical limits and design principle for plant and fungal movements. Science 308:1308–10.

Stamp NE. 1984. Self-burial behaviour of *Erodium cicutarium* seeds. J Ecol 72:611–20.

Wahl AM. 1963. Mechanical springs. 2nd ed. New York (NY): McGraw-Hill.

Weintraub M. 1952. Leaf movements in Mimosa pudica L. New Phytol 50:357–82.

Wentworth CK. 1922. A scale of grade and class terms for clastic sediments. J Geol 30:377–92.

Winter AG, Deits RLH, Hosoi AE. 2012. Localized fluidization burrowing mechanics of *Ensis directus*. J Exp Biol 215:2072–80.